



Cite this: *Chem. Sci.*, 2023, **14**, 5894

All publication charges for this article have been paid for by the Royal Society of Chemistry

Received 23rd March 2023
 Accepted 25th April 2023

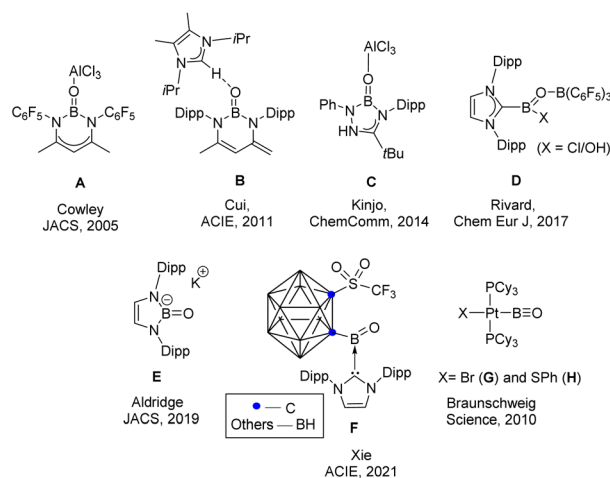
DOI: 10.1039/d3sc01544k
rsc.li/chemical-science

Introduction

The parent oxaborane, HBO is a compound that features boron with both a $-B=O$ and a $B-H$ functional group. This ephemeral compound has only been detected in the gas phase or by low-temperature matrix isolation studies.¹ Significant effort has recently been focused on generating oxaborane derivatives RBO. The first report of a $B=O$ double bond (**A**) came from Cowley's group in 2005.² Subsequently, the concept of donor/acceptor stabilization has been successfully employed by the groups of Cui, Kinjo, Rivard, and others (Scheme 1) to generate compounds with $B=O$ double bonds (**B–D**).^{3–5} The groups of Aldridge and Xie were able to isolate an acid-free, anionic and neutral $B=O$ doubly bound species, respectively (**E & F**).^{6,7} Braunschweig and coworkers adopted a different strategy for the isolation of multiply bound boron compounds by trapping them within the coordination sphere of a transition metal,^{8–10} and they were able to isolate the compounds with a $B\equiv O$ triple bond (**G & H**).¹¹ Last year, Braunschweig and coworkers isolated a base-stabilized derivative of the parent borylene carbonyl ($HB=C=O$) and provided substantial evidence of the

intermediacy of base-stabilized ($cAACB(H)=O$; $cAAC$ = cyclic alkyl amino carbene) and base-free oxaboranes ($RB\equiv O$) and these reported intermediates are also “parent” oxaboranes.¹² Inspired by these reports, we wondered whether a parent oxaborane [$LB(H)=O$] could be isolated ($L=6$ -SIDipp; 6 -SIDipp = $1,3$ -di(2,6-diisopropylphenyl)tetrahydropyrimidine-2-ylidene) and how the dominant cyclization reaction could be circumvented.

Recently, a wide range of N-heterocyclic carbenes (NHCs) and cyclic alkyl amino carbenes ($cAACs$) have been utilized to form stable adducts with BH_3 , thanks to the initial works of Robinson¹³ and later from the groups of Fensterbank, Lacôte,



Scheme 1 Examples of previously reported oxaborane and a compound with a $B=O$ triple bond. The parent oxaborane is still elusive.

^aInorganic Chemistry and Catalysis Division, CSIR-National Chemical Laboratory, Dr Homi Bhabha Road, Pashan, Pune 411008, India. E-mail: ss.sen@ncl.res.in

^bAcademy of Scientific and Innovative Research (AcSIR), Ghaziabad 201002, India

^cPhysical and Material Chemistry Division, CSIR-National Chemical Laboratory, Dr Homi Bhabha Road, Pashan, Pune 411008, India

^dAnalytical and Environmental Sciences Division and Centralized Instrumentation Facility, CSIR-Central Salt and Marine Chemicals Research Institute, Gijubhai Badheka Marg, Bhavnagar-364002, India

† Electronic supplementary information (ESI) available: Experimental details, spectroscopic data, theoretical calculations, and representative NMR spectra. CCDC 2234583 (**1**), 2234584 (**2**) and 2234585 (**3**). For ESI and crystallographic data in CIF or other electronic format see DOI: <https://doi.org/10.1039/d3sc01544k>



Malacria, Curran, Braunschweig, and others.^{14,15} This has resulted in applications in the borylation of aromatic or aliphatic C–H bonds, the hydroboration of alkenes, and many other organic transformation.¹⁶ Beginning of the last year, we became interested in employing 6-SIDipp as a ligand in borane chemistry. We demonstrated substitution reactions of 6-SIDipp·BH₃, ring expansion with 6-SIDipp·9BBN, and activation of the B–H bond of HBpin with 6-SIDipp.^{17–19} These studies have indicated that 6-SNHC has a notably higher donating capacity than 5-NHC. Our hypothesis was that by incorporating the 6-SNHC framework, along with bulky Dipp groups, and using a Lewis acid, we could potentially achieve the isolation of a single, parent oxaborane molecule.

Results and discussion

The groups of Vedejs and Curran attempted to synthesize the dihydrido borenium cation, [5-IDipp→BH₂]⁺ starting from 5-Dipp·BH₃ [IDipp = 1,3-bis(2,6-diisopropylphenyl)-imidazole-2-ylidene] and AlCl₃, but they observed the formation of a cationic hydride-bridged dimer as an intermediate (Scheme 2).²⁰ The latter was not isolated and [5-IDipp·BCl₂]⁺ was obtained as the final product. However, such hydride-bridged dimer was reported by the Vedejs group by the treatment of R₃N·BH₃ with [Ph₃C][B(C₆F₅)₃]²¹ and by Alcarazo and coworkers upon reaction with 5-IDipp·BH₃ with B(C₆F₅)₃.²² The reaction of 6-SIDipp·BH₃ with 1.2 equivalent of gallium trichloride in toluene at room temperature resulted in complete disappearance of the ¹¹B{¹H} NMR quartet of 6-SIDipp·BH₃ at -31.3 ppm ($J_{B-H} = 84.1$ Hz)¹⁷ and the appearance of a new multiplet at -27.4 ppm ($J_{B-H} = 72.1$ Hz), which is in good agreement with several NHC-supported boronium cations.^{22,23} Single crystal X-ray studies confirm the constitution of **1** (Fig. 1). The B–H–Ga binding mode in **1** can be best described as a three-center two-electron (3c–2e) bond. The location of the two bridging hydrogens and a single terminal hydrogen in each could be inferred from the difference Fourier map. The C1–B1 distance in **1** is 1.596(6) Å, which is good agreement with that in 6-SIDipp·BH₃ [1.602(3) Å].¹⁷ The terminal B–H bond distance [1.10(4) Å] is slightly

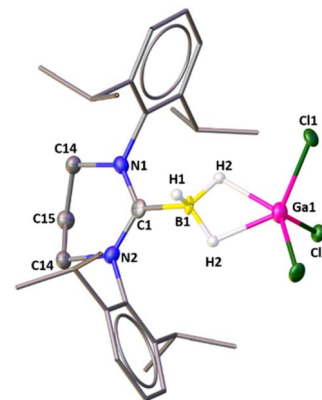


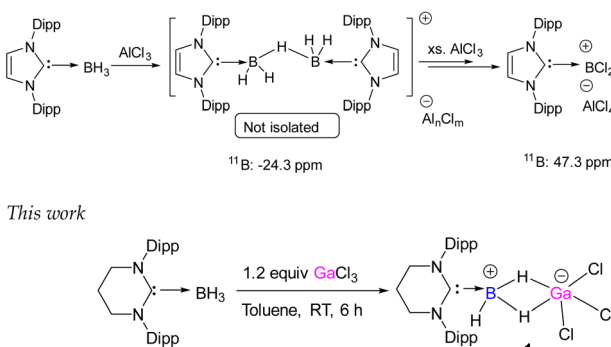
Fig. 1 The molecular structure of **1**. Hydrogen atoms (except the hydrogens attached with boron atom) are omitted for clarity. Selected bond distances (Å), bond angles (deg), and torsion angle (deg): C1–N1 1.337(3), C1–N2 1.337(3), B1–C1 1.596(6), B1–H1 1.10(4), B1–H2 1.08(3), Ga1···B1 2.280(5), Ga1–H2 1.83(3), Ga–Cl1 2.1755(8); N1–C1–N2 119.3(3), N2–C1–B1 120.29(16), N1–C1–B1 120.29(16), C1–B1–H2 112.3(17), C1–B1–H1 112(2).

longer than those of bridging B–H bonds [1.08(3) Å]. The B–Ga distance for **1** is 2.280(5) Å, which is longer than the reported B–Ga coordinate bond in HC[MeC(2,6-iPr₂C₆H₃)N]₂Ga→B(C₆F₅)₃ [2.156(1) and 2.142(3) Å],²⁴ indicating the absence of any interaction between boron and the gallium center. The Ga–H bond distance is 1.83(3) Å, which is slightly shorter than in the Ga–H–Ga bridges.²⁵ The geometry of the boron atom is distorted tetrahedral, while the gallium atom adopts a trigonal bipyramidal geometry.

In order to investigate the electronic structure of compound **1**, density functional theory (DFT) calculations were performed. The B3LYP functional and the def2-TZVP basis set have been employed in the calculations (please see the ESI† for further details). The NBO analysis shows that there are two significant electron donations from the BD orbital (which denotes a bonding orbital) of the B1–H2 bond to the vacant s and p orbitals of gallium in **1**, with stabilization energies of 24.3 kcal mol⁻¹ and 27.6 kcal mol⁻¹ (see Fig. S17†). Similarly, the BD orbital of the second B–H bond (which is identically denoted as B1–H2 in Fig. 2) also shows two significant electron donations to the vacant s and p orbitals of gallium, with identical (to that of the first B–H bond) stabilization energies of 24.3 kcal mol⁻¹ and 27.6 kcal mol⁻¹ (see Fig. S17†). It should be noted that the NBO analysis in this case resulted in a misinterpretation of the nature of the Ga–Cl bonds as ionic instead of covalent, due to the limitations in NBO in accurately locating polar bonds. Conceptually, the B–H bonding orbitals can donate electron density to either an initially vacant p orbital located on Ga or to a Ga–Cl σ* antibonding orbital, in which the lobe is predominantly located on Ga. This corroborates the experimental observation of two identical B–H bonds and also suggests a 3c–2e bond character in B–H–Ga interactions.

Boranes have been identified as promising candidates for facilitating hydrogen release from water, as documented in several early microwave spectroscopic studies, and theoretical

Curran and vedejs, JACS, 2013



Scheme 2 Diverse reactivity of NHC·BH₃. The upper scheme describes the generation of 5-IDipp·BCl₂ cation. The lower scheme shows the synthesis of boron–gallium 3c–2e complex (**1**).



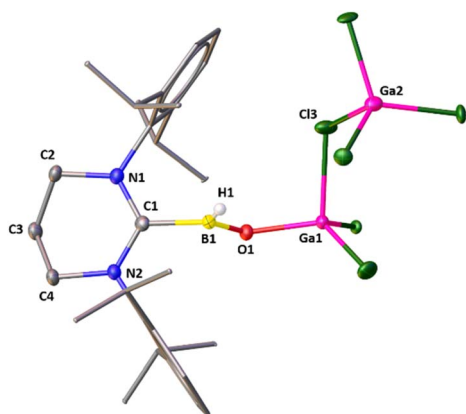


Fig. 2 The molecular structure of $2 \cdot \text{GaCl}_3$. Hydrogen atoms (except the hydrogen attached with boron atom) are omitted for clarity. Selected bond distances (\AA), bond angles (deg), and torsion angle (deg): C1–N1 1.328(3), C1–N2 1.328(3), B1–C1 1.621(4), B1–O1 1.307(3), B1–H1 1.09(3), Ga1–O1 1.807(2), Ga1–Cl13 2.3015(10); N1–C1–N2 122.1(2), N1–C1–B1 118.5(2), C1–B1–O1 118.3(2), C1–B1–H1 117.6(17), B1–O1–Ga1 127.97(18), Ga1–Cl13–Ga2 117.49(4).

calculations.²⁶ It is known that BH_3 reacts with H_2O to give $\text{B}(\text{OH})_3$ with concomitant dihydrogen liberation. Recently, Kraka and co-workers investigated the mechanism of H_2 release from BH_3 in water and demonstrated that one H_2O molecule interacting with BH_3 led to an activation energy of 24.9 kcal mol⁻¹.²⁷

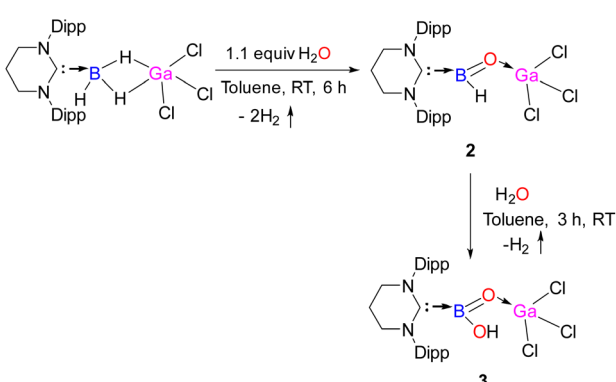
We have reacted **1** with 1.1 equivalent of H_2O , which resulted in the formation of **2** with simultaneous elimination of dihydrogen (Scheme 3). **2** is a heterodinuclear compound that can be considered as the acid-stabilized parent oxaborane containing an unusual $\text{H}(\text{B}=\text{O})$ linkage. The elimination of dihydrogen was detected using NMR spectroscopy and GC-MS. The amount of simultaneous hydrogen production is quite large (2.1 mmol h⁻¹ g⁻¹). Most importantly, the NHC moiety remained intact during the reaction, which was not the case for 5-IDipp· BH_2I and 5-IDipp· BH_2OTf as their reactions with water (or methanol) resulted in fast hydrolysis (or methanolysis) to the corresponding imidazolium salts.²⁸ The $^{11}\text{B}\{^1\text{H}\}$ NMR spectrum of **2** displays a broad signal at 21.6 ppm for the $\text{B}=\text{O}$

moiety, which falls in the range of 19.7–32.3 ppm, typically found in oxaboranes. The characteristic terminal $\nu(\text{B}=\text{O})$ stretch frequency appeared at 1665 cm^{-1} for **2**, which is in good agreement with the previously reported oxaboranes (1558–1646 cm^{-1}).^{5,6}

Attempts to crystallize **2** resulted in two types of colorless single crystals: one is block shaped, and the other one is needle shaped. While the needle shaped crystals belong to **2**, the block shaped crystals account for $2 \cdot \text{GaCl}_3$. Though the constitution and the connectivity of **2** can be unambiguously established from the single crystal X-ray data (Fig. S16, ESI†), we refrain from a discussion of bonding parameters because of the low quality of the data. The molecular structure of $2 \cdot \text{GaCl}_3$ is displayed in Fig. 2. One of the GaCl_3 molecule cocrystallizes with **2**. The main feature of $2 \cdot \text{GaCl}_3$ is that the central boron atom has bonded to one terminal hydrogen atom and oxygen atom which is connected to the gallium center. The boron atom exhibits a highly distorted trigonal planar coordination site with the carbon atom of NHC, the hydride ligand, and the (μ -O) atom. The gallium atom has a distorted tetrahedral coordination sphere comprised of the (μ -O) atom and the three chloride ligands. The B–H [1.09 (3) \AA] and B–C [1.621(4) \AA] bond lengths compare well with their typical bond lengths. It is noted that the B=O distance in $2 \cdot \text{GaCl}_3$ [1.307(3) \AA] is in good agreement with the reported acid stabilized oxaboranes,^{3–6} slightly longer compared to Aldridge's acid free anionic oxaboranes [1.256(3) \AA , 1.273(8) \AA and 1.287 (2) \AA],⁷ and substantially longer than Braunschweig's B≡O triply bound complex.¹¹ The Ga–O bond length in $2 \cdot \text{GaCl}_3$ [1.807(2) \AA] is in good agreement with that in Roesky's Ga(Me)–O–Bi linkage [1.815(13) \AA .²⁹

Having found that water undergoes facile dehydrocoupling with the bridging hydride of **1**, it seemed plausible that further addition of H_2O may lead to the release of another molecule of H_2 and convert the terminal B–H bond to a B–OH bond to generate a (hydroxy)oxaborane. Gratifyingly, the reaction of **2** with another molecule of H_2O led to the formation of **3** containing a $\text{B}(\text{OH})=\text{O} \cdot \text{GaCl}_3$ motif with concomitant elimination of H_2 (Scheme 3). The NHC moiety and the ($\text{B}=\text{O}$)– GaCl_3 remained intact, while the B–H bond underwent hydrolysis with H_2O to generate the terminal B–OH bond. **3** possesses a rare unit of $[\text{B}(\text{OH})=\text{O}]$, and it is the second example of a monomeric boracarboxylic acid complex that has been isolated, followed by Rivard's discovery of **D**.⁵ The $[\text{B}(\text{OH})=\text{O}]$ unit is transient and can only be observed in the gas phase during the thermal conversion of orthoboric acid ($\text{B}(\text{OH})_3$) to metaboric acid $[(\text{HOBO})_3]$.³⁰ The boron atom resonates at 23.6 ppm. The solid-state structure of **3** is displayed in Fig. 3. The terminal B–O bond length [1.334(10) \AA] in **3** is very similar with the B–O double bond [1.320(9) \AA] as they overlap within three times of estimated standard deviation. For a note, the B–O double bond in **3** is also comparable to that in **2** [1.307(3) \AA]. The characteristic terminal $\nu(\text{B}=\text{O})$ stretching frequency of **3** appeared at 1595 cm^{-1} .

To investigate the electronic structure of **2** and **3**, density functional theory (DFT) calculations were performed. The B3LYP functional and the def2-TZVP basis set have been employed in the calculations (see the ESI† for further details).



Scheme 3 Stepwise synthesis of -hydrido and -hydroxy oxaboranes, **2** and **3** from the reaction of **1** with water.



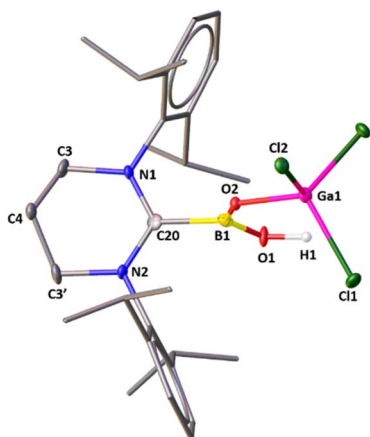


Fig. 3 The molecular structure of 3. Hydrogen atoms (except the hydrogens attached with oxygen atom) are omitted for clarity. Selected bond distances (Å), bond angles (deg), and torsion angle (deg): C20–N1 1.334(5), B1–C20 1.631(9), B1–O2 1.320(9), B1–O1 1.334(10), O1–H1 0.97(2), O2–Ga1 1.822(5), Ga1–Cl1 2.1803(14), Ga1–Cl2 2.159(2); N1–C20–N2 120.4(6), N1–C20–B1 119.7(3), O1–B1–O2 130.2(7), B1–O2–Ga1 131.1(5), Cl2–Ga1–Cl2 111.74(5).

The Wiberg Bond Index (WBI) of the B–O bond in 2 was determined to be 1.19. Moreover, the natural population analysis (NPA) charges on B and O were found to be +0.77 and –1.04, respectively, indicating a multiple bond character of the B–O bond, which is polarized towards oxygen. Similarly, the Wiberg Bond Index (WBI) of the B–O bond in compound 3 is 1.09, which is slightly lower than that of compound 2, indicating a weaker B–O bond in compound 3. The natural population analysis (NPA) charges on B and O were determined to be +1.08 and –1.06, respectively. The higher positive charge on the boron atom in compound 3 is likely due to its bonding with two oxygen atoms, in contrast to one oxygen and one hydrogen in compound 2.

Furthermore, the NBO analysis shows a significant electron donation from the LP orbital (which denotes a lone pair orbital) of oxygen to the vacant p orbital of boron in 2, with a stabilization energy of 85.4 kcal mol^{–1} (see Fig. 4). This indicates

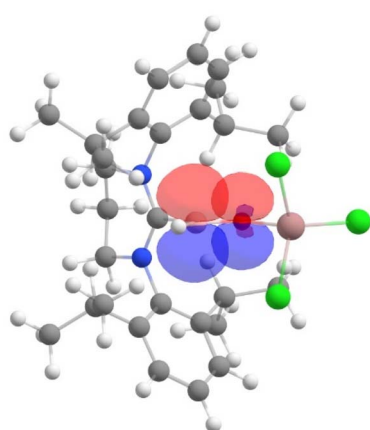


Fig. 4 The NBO plot of the desired intramolecular donor–acceptor interactions (LP orbital of oxygen to vacant p orbital of boron) in 2.

significant B–O π bonding. In the case of 3, the corresponding interaction was weaker, with a stabilization energy of 66.1 kcal mol^{–1} (see Fig. S18†), indicating a weaker π bonding interaction between boron and oxygen in 3 compared to 2.

Conclusions

In summary, we synthesized the first parent oxaborane derivative (2) by adopting the textbook reaction of BH₃ with water. We accessed 2 by reacting an unusual 3c–2e boron–gallium compound (1) with water as an oxygen source, with concomitant elimination of H₂. The strong σ-donation from 6-SIDipp and coordination of the B=O unit to gallium can be attributed for the stabilization of 2. Further reaction of 2 with another molecule of water resulted in a bora-carboxylic acid derivative (3), which is a monomer of metaboric acid. Investigation of the reactivity 2 and synthesis of other multiply bound boron compounds is underway in our laboratory, and will be published in due course.

Data availability

Synthetic details and analytical data, including depictions of all spectra and detailed accounts on the methods applied are documented in the ESI.† Crystallographic data are made available *via* the CCDC. Coordinate data of all computationally optimised species are provided as a separate xyz-file in the ESI.†

Author contributions

G. K. and S. S. S. conceived the idea. G. K. and P. R. A. have carried out all the experiments. G. K. and S. T. performed the single-crystal XRD measurements. K. V. R. and K. V. have performed the theoretical calculations. All the authors have contributed in writing the manuscript.

Conflicts of interest

There are no conflicts to declare.

Acknowledgements

S. S. S. is thankful for SJF Grant SB/SJF/2021-22/06, GOI for providing financial assistance. G. K. and K. V. R. thank CSIR, India for their research fellowships. K. V. and P. R. A. are grateful to the CSIR-FIRST scheme for providing financial assistance. S. T. is grateful to AESD&CIF, CSIR-CSMCRI for instrumentation facilities and infrastructure. The support and the resources provided by 'PARAM Brahma Facility' under the National Supercomputing Mission, Government of India at the Indian Institute of Science Education and Research (IISER) Pune are gratefully acknowledged.

Notes and references

- (a) B. Pachaly and R. West, *J. Am. Chem. Soc.*, 1985, **107**, 2987–2988; (b) P. Paetzold, S. Neyses and L. Geret, *Z. Anorg. Allg. Chem.*



Chem., 1995, **621**, 732–736; (c) M. Ito, N. Tokitoh and R. Okazaki, *Tetrahedron Lett.*, 1997, **38**, 4451–4454; (d) S. A. Wescott, *Angew. Chem., Int. Ed.*, 2010, **49**, 9045–9046.

2 D. Vidovic, J. A. Moore, J. N. Jones and A. H. Cowley, *J. Am. Chem. Soc.*, 2005, **127**, 4566–4567.

3 Y. Wang, H. Hu, J. Zhang and C. Cui, *Angew. Chem., Int. Ed.*, 2011, **50**, 2816–2819.

4 Y. K. Loh, C. C. Chong, R. Ganguly, Y. Li, D. Vidovic and R. Kinjo, *Chem. Commun.*, 2014, **50**, 8561–8564.

5 A. K. Swarnakar, C. Hering-Junghans, M. J. Ferguson, R. McDonald and E. Rivard, *Chem.-Eur. J.*, 2017, **23**, 8628–8631.

6 H. Wang, J. Zhang, J. Yang and Z. Xie, *Angew. Chem., Int. Ed.*, 2021, **60**, 19008–19012.

7 Y. K. Loh, K. Porteous, M. Á. Fuentes, D. C. H. Do, J. Hicks and S. Aldridge, *J. Am. Chem. Soc.*, 2019, **141**, 8073–8077.

8 H. Braunschweig, K. Radacki, D. Rais and K. Uttinger, *Angew. Chem., Int. Ed.*, 2006, **45**, 162–165.

9 J. Brand, H. Braunschweig, F. Hupp, A. K. Phukan, K. Radacki and S. S. Sen, *Angew. Chem., Int. Ed.*, 2014, **53**, 2240–2244.

10 T. E. Stennett, J. D. Mattock, I. Vollert, A. Vargas and H. Braunschweig, *Angew. Chem., Int. Ed.*, 2018, **57**, 4098–4102.

11 H. Braunschweig, K. Radacki and A. Schneider, *Science*, 2010, **328**, 345–347.

12 A. Stoy, M. Härterich, R. D. Dewhurst, J. O. C. Jiménez-Halla, P. Endres, M. Eyßlein, T. Kupfer, A. Deissenberger, T. Thiess and H. Braunschweig, *J. Am. Chem. Soc.*, 2022, **144**, 3376–3380.

13 Y. Wang, B. Quillian, P. Wei, C. S. Wannere, Y. Xie, R. B. King, H. F. Schaefer III, P. v. R. Schleyer and G. H. Robinson, *J. Am. Chem. Soc.*, 2007, **129**, 12412–12413.

14 (a) S.-H. Ueng, M. M. Brahmi, É. Derat, L. Fensterbank, E. Lacôte, M. Malacria and D. P. Curran, *J. Am. Chem. Soc.*, 2008, **130**, 10082–10083; (b) M. M. Brahmi, J. Monot, M. D.-E. Murr, D. P. Curran, L. Fensterbank, E. Lacôte and M. Malacria, *J. Org. Chem.*, 2010, **75**, 6983–6985; (c) A. Solovyev, Q. Chu, S. J. Geib, L. Fensterbank, M. Malacria, E. Lacôte and D. P. Curran, *J. Am. Chem. Soc.*, 2010, **132**, 15072–15080; (d) W. Dai, S. J. Geib and D. P. Curran, *J. Org. Chem.*, 2018, **83**, 8775–8779; (e) D. P. Curran, A. Solovyev, M. M. Brahmi, L. Fensterbank, M. Malacria and E. Lacôte, *Angew. Chem., Int. Ed.*, 2011, **50**, 10294–10317.

15 D. Auerhammer, M. Arrowsmith, H. Braunschweig, R. D. Dewhurst, J. O. C. Jiménez-Halla and T. Kupfer, *Chem. Sci.*, 2017, **8**, 7066–7071.

16 (a) A. Prokofjevs, A. Boussonnière, L. Li, H. Bonin, E. Lacôte, D. P. Curran and E. Vedejs, *J. Am. Chem. Soc.*, 2012, **134**, 12281–12288; (b) A. Prokofjevs and E. Vedejs, *J. Am. Chem. Soc.*, 2011, **133**, 20056–20059.

17 G. Kundu, V. S. Ajithkumar, K. V. Raj, K. Vanka, S. Tothadi and S. S. Sen, *Chem. Commun.*, 2022, **58**, 3783–3786.

18 G. Kundu, K. Balayan, S. Tothadi and S. S. Sen, *Inorg. Chem.*, 2022, **61**, 12991–12997.

19 G. Kundu, R. Dixit, S. Tothadi, K. Vanka and S. S. Sen, *Dalton Trans.*, 2022, **51**, 14452–14457.

20 A. Prokofjevs, J. W. Kampf, A. Solovyev, D. P. Curran and E. Vedejs, *J. Am. Chem. Soc.*, 2013, **135**, 15686–15689.

21 T. S. De Vries and E. Vedejs, *Organometallics*, 2007, **26**, 3079–3081.

22 B. Inés, M. Patil, J. Carreras, R. Goddard, W. Thiel and M. Alcarazo, *Angew. Chem., Int. Ed.*, 2011, **50**, 8400–8403.

23 C. Chen, J. Li, C. G. Daniliuc, C. Mück-Lichtenfeld, G. Kehr and G. Erker, *Angew. Chem., Int. Ed.*, 2020, **59**, 21460–21464.

24 (a) N. J. Hardman, P. P. Power, J. D. Gorden, C. L. B. Macdonald and A. H. Cowley, *Chem. Commun.*, 2001, 1866–1867; (b) N. Dettenrieder, C. Schädle, C. Maichle-Mössmer, P. Sirsch and R. Anwander, *J. Am. Chem. Soc.*, 2014, **136**, 886–889.

25 (a) C. R. Pulham, A. J. Downs, M. J. Goode, D. W. H. Rankin and H. E. Robertson, *J. Am. Chem. Soc.*, 1991, **113**, 5149–5162; (b) A. J. Downs, S. Parsons, C. R. Pulham and P. F. Souter, *Angew. Chem., Int. Ed. Engl.*, 1997, **36**, 890–891.

26 S. Swinnen, V. S. Nguyen, S. Sakai and M. T. Nguyen, *Chem. Phys. Lett.*, 2009, **472**, 175–180.

27 S. Nanayakkara, M. Freindorf, Y. Tao and E. Kraka, *J. Phys. Chem. A*, 2020, **124**, 8978–8993.

28 https://d-scholarship.pitt.edu/10833/1/Andrey_Solovyev_PhD_Dissertation_2012.pdf.

29 B. Nekoueishahraki, A. Jana, H. W. Roesky, L. Mishra, D. Stern and D. Stalke, *Organometallics*, 2009, **28**, 5733–5738.

30 (a) L. Andrews and T. R. Burkholder, *J. Chem. Phys.*, 1992, **97**, 7203; (b) D. White, D. E. Mann, P. N. Walsh and A. Sommer, *J. Chem. Phys.*, 1960, **32**, 488.

